Journal of Magnetics 15(1), 21-24 (2010) DOI: 10.4283/JMAG.2010.15.1.021

Magnetic Property of α-Fe_2O_3 Nanoparticles Prepared by Sonochemistry and Take-off Technique

Y. S. Koo, B. K. Yun, and J. H. Jung*

Department of Physics, Inha University, Incheon 402-751, Korea

(Received 9 November 2009, Received in final form 14 December 2009, Accepted 29 December 2009)

A new synthetic method for the formation of uniform α-Fe_2O_3 nanoparticles was reported and their magnetic properties were investigated. The sonochemical synthesis and the subsequent take-off technique resulted in spherical shaped α-Fe_2O_3 nanoparticles with an average diameter of 60 nm. The temperature- and applied magnetic field-dependent magnetization of the α-Fe_2O_3 nanoparticles was explained by the sum of two contributions, i.e., the Morin transition and superparamagnetism, because the critical size for superparamagnetism was within the size variation of the nanoparticles.

Keywords : sonochemical synthesis, α-Fe_2O_3, Morin transition, superparamagnetism

1. Introduction

Transition metal oxides have drawn considerable interest because their magnetic properties subtly change depending on their size [1, 2]. Among the binary iron oxides, α-Fe_2O_3 (hematite) exhibits antiferromagnetism (below T_N ~960 K) and an intriguing Morin transition (T_M~263 K) [3]. The spins are antiferromagnetically aligned along the trigonal [111] axis (c-axis) below the T_M while the spins are slightly tilted within the basal (111) plane (c-plane), and a small net magnetic moment appears (weak ferromagnetism) above the T_M. From theoretical analysis [4], T_M is determined by the competition between the magnetic dipolar and the fine structure magneto-crystalline anisotropies.

Many reports have examined the changes in the magnetic properties and/or the Morin transition of α-Fe_2O_3 nanoparticles [5-7]. Until now, most of the reports have used α-Fe_2O_3 nanoparticles that were synthesized through a chemical route and subsequent heat treated at temperature of less than 500 °C. Although this low temperature heat treatment is inevitable for the formation of nanoparticle in order to prevent aggregation, low temperature heat treatment usually results in a low crystalline quality and sometimes amorphous nanoparticles [8]. A new method must be developed to synthesize highly crystalline α-Fe_2O_3 nanoparticles with a uniform size and shape because the geometrical factors, such as the size and shape, and the crystalline quality strongly affect the magnetic properties.

In this work, the magnetic properties were examined for α-Fe_2O_3 nanoparticles that were synthesized using a sonochemical method with a subsequent heat treatment at 800 °C and a take-off technique. α-Fe_2O_3 did not aggregate even during this high temperature heat treatment because of the chemical bonding between α-Fe_2O_3 and $BaTiO_3$. The temperature and applied magnetic field dependences of the magnetization of these α-Fe_2O_3 nanoparticles were explained by the sum of two contributions, i.e., the Morin transition and superparamagnetism.

2. Experiments

Three steps were used to prepare the α-Fe_2O_3 nanoparticles with a narrow size distribution. First, the Fe_3O_4 nanoparticles (~50 nm in diameter) were plated onto the surface of $BaTiO_3$ (~500 nm in diameter) using a sonochemical method, that was similar to the methods described in Previous works [9, 10]. The reaction time and pH were controlled in order to separate the Fe_3O_4 nanoparticles from each other on the $BaTiO_3$ surface. Fe_3O_4 was transformed into α-Fe_2O_3 through the heat treatment at 800 °C for 24 hours in an oxygen environment, as described in a previous report [11]. Finally, an ultrasonic wave (750 W, 20 kHz) was used to remove the α-Fe_2O_3 nanoparticles from $BaTiO_3$. These α-Fe_2O_3 nanoparticles were washed

*Corresponding author: Tel: +82-32-860-7659
Fax: +82-32-872-7562, e-mail: jhjung@inha.ac.kr

and filtered several times and then dried at 110 °C for 24 hours. When the same steps were used except for the plating step for Fe_3O_4 on the surface of $BaTiO_3$, the α-Fe_2O_3 bulk (not nanoparticle) was easily formed probably because of the aggregation of α-Fe_2O_3 during the heat treatment process at high temperatures.

The microstructure and the particle size of the α-Fe_2O_3 nanoparticles were examined using a transmission electron microscope and dynamic light scattering analysis measurements, respectively. The phase and crystalline quality were characterized using x-ray diffraction (XRD) measurements with Cu $K\alpha$ radiation. The magnetic property measurements were performed using a vibrating sample magnetometer (VSM) in a physical property measurement system (Quantum design, PPMS).

3. Results and Discussion

Figure 1 shows the x-ray diffraction pattern of the α-Fe_2O_3 nanoparticles (a solid line) near the (104) and (110) planes. [For comparison purposes, the diffraction pattern of the α-Fe_2O_3 bulk (a dashed line) is also shown.] Compared to the α-Fe_2O_3 bulk peaks, the α-Fe_2O_3 nanoparticle peaks were rather broad because of their smaller grain size. Additionally, the α-Fe_2O_3 nanoparticle peaks were located at lower angles, suggesting that the lattice constants were elongated. The lattice constants of the nanoparticles were estimated to be a = 5.036 Å and c = 13.726 Å from the (104) and (110) diffraction peaks, whereas the lattice constants of the bulk were a = 5.025 Å and c = 13.716 Å.

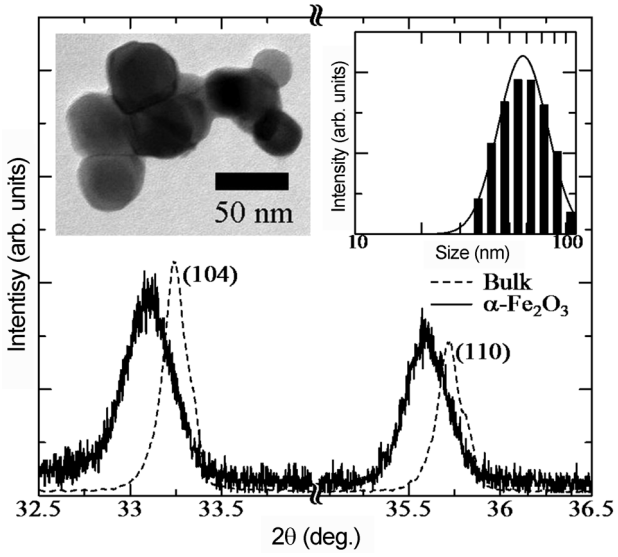

Fig. 1. X-ray diffraction pattern of the α-Fe_2O_3 nanoparticles (a solid line) and the bulk (a dashed line) near the (104) and (110) planes. the transmission electron microscope image and the distribution of particle size are shown in the left and right insets, respectively. In the right inset, the solid line represents the log-normal functional fitting.

The size and the shape of the α-Fe_2O_3 nanoparticles strongly depend on the synthesis method [12]. In a previous report, α-Fe_2O_3 nanoparticles that were synthesized using a similar sonochemical method and a heat treatment at 570 °C exhibited an ellipsoidal shape with an average length of 30 nm and a mean diameter of 18 nm [13]. In this study, the transmission electron microscope image and the distribution of the particle size of the α-Fe_2O_3 nanoparticles are shown in the left and right insets of Fig. 1, respectively. Distinctively, the α-Fe_2O_3 nanoparticles that were synthesized using the sonochemical method and the take-off technique exhibited a spherical shape with an average particle size of 60 nm.

Figure 2 shows the zero-field-cooled (ZFC) and fthe ield-cooled (FC) magnetization curves of the α-Fe_2O_3 nanoparticle (solid lines). [The magnetization curves were normalized using the magnetization value at 350 K in order to directly compare the magnetization curves of the α-Fe_2O_3 bulk (dashed lines).] The α-Fe_2O_3 bulk clearly exhibited a first-order Morin transition near $T_{M,B}$~250 K with a large hysteresis (see, the inset). The magnetization was finite above the $T_{M,B}$ and negligible below the $T_{M,B}$ with little variation with respect to temperature changes. On the other hand, the α-Fe_2O_3 nanoparticle exhibited a first-order Morin transition with quite broad temperature range near the $T_{M,N}$~200 K (see, the inset). Both above and below the $T_{M,N}$, the magnetization exhibited irrever-

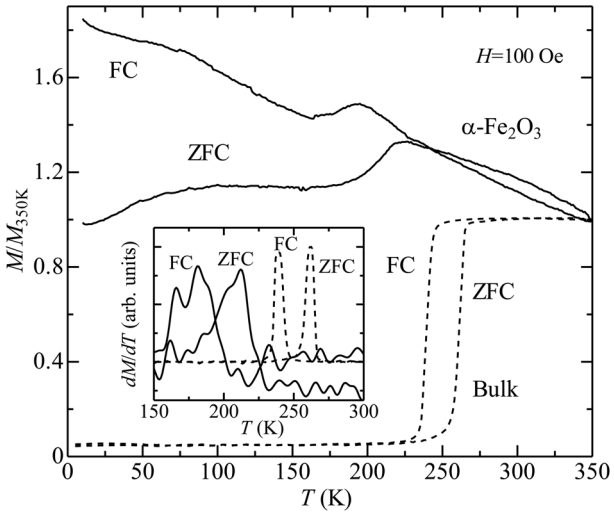

Fig. 2. The zero-field-cooled (ZFC) and the field-cooled (FC) magnetization curves of the α-Fe_2O_3 nanoparticles (solid lines) and the bulk (dashed lines). The differentiated magnetization curves near the Morin transition temperature are shown in the inset.

sible behaviors between the ZFC and the FC. Additionally, the magnetization did not drastically change near the $T_{M,N}$.

The Morin transition temperature is determined by the competition between the magnetic dipolar anisotropy and the fine structure anisotropy. The former cause the spins to lie in the *c*-plane, whereas the latter aligns the spins along the *c*-axis. In the α-Fe_2O_3 nanoparticles, the magnetic dipolar anisotropy increased because of the large number of surface spins, whereas the fine structure anisotropy decreased because the existence of defects and vacancies [14]. Although the magnetic dipole anisotropy decreased because of the enlarged lattice constant, this effect was not as significant as the other two effects. Therefore, the T_M of the α-Fe_2O_3 nanoparticles was lower than the bulk.

Below the $T_{M,N}$, the ZFC and FC magnetizations of the α-Fe_2O_3 nanoparticle changed at another characteristic temperature. The ZFC magnetization decreased with a broad peak as the temperature, whereas the FC magnetization increased with a change in the slope of nearly 100 K. these ZFC and FC behaviors corresponded to superparamagnetism, which has been observed in the α-Fe_2O_3 nanoparticles [15]. Superparamagnetism is characterized by fluctuations in the magnetic domain because of thermal agitation above the blocking temperature T_B (~100 K), and a spatially frozen domain below the T_B. The ZFC magnetization of the α-Fe_2O_3 nanoparticles was flat in the temperature range of 100 K ~ 200 K because of the contributions from the antiferromagnetic Morin transition and superparamagnetism.

Figures 3 (a)~(d) show the magnetic hysteresis loops (solid lines) of the α-Fe_2O_3 nanoparticles at 280 K ($>T_{M,N}$), 220 K ($\sim T_{M,N}$), 140 K ($T_{M,N} > T > T_B$), and 5 K ($<T_B$), respectively. [For comparison purposes, the magnetic hysteresis loops of the α-Fe_2O_3 bulk (dashed lines) are also shown.] The absolute value of the magnetization for the α-Fe_2O_3 nanoparticles was rather small because of the imperfect separation of α-Fe_2O_3 from $BaTiO_3$. However, the nonmagnetic $BaTiO_3$ did not affect the magnetic properties of the α-Fe_2O_3 nanoparticles.

Above the $T_{M,N}$, both the *M-H* curves of the α-Fe_2O_3 nanoparticles and the bulk exhibited hysteresis loops. The *M-H* curve of the α-Fe_2O_3 nanoparticles had a smaller coercive field than the bulk probably because of the smaller magnetic domain size, the *M-H* curve near H=0 T was slightly deformed because of the spherical shape of the α-Fe_2O_3 nanoparticles, similar to a previous report [6]. Near the $T_{M,N}$, the *M-H* curve of the α-Fe_2O_3 bulk exhibited a linear behavior because of its antiferromagnetism. However, the *M-H* curve of the α-Fe_2O_3 nanoparticles exhibited a hysteresis loop. From $T_{M,N} > T > T_B$, the *M-H* curve of the α-Fe_2O_3 nanoparticles possessed a clear hysteresis loop, not a linear behavior. Additionally, the magnetic moment at 2 T and 140 K was larger than at 220 K. Below the T_B, the *M-H* curve of the α-Fe_2O_3 nanoparticles exhibited a large remanent magnetization as well as a large coercive field. [The magnetization at 5 K was divided by two for clarity.] Additionally, the magnetic hysteresis loop was not closed even at H=2 T.

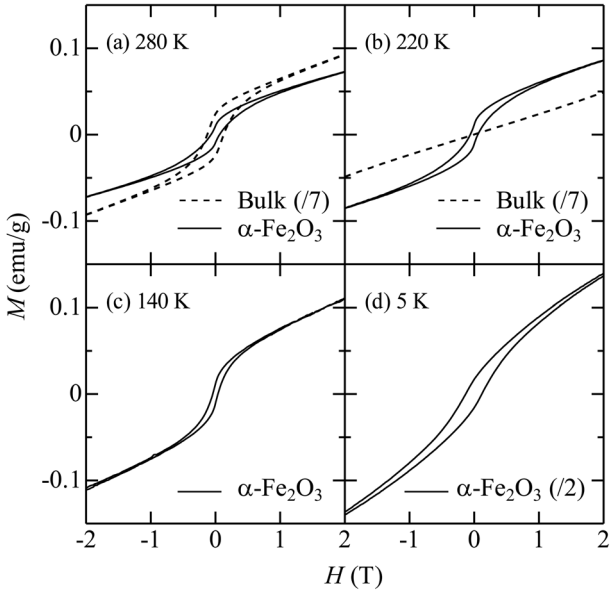

Fig. 3. Magnetic hysteresis loops (solid lines) of the α-Fe_2O_3 nanoparticles at (a) 280 K, (b) 220 K, (c) 140 K, and (d) 5 K. The value of the magnetization at 5 K was divided by two for clarity. The magnetic hysteresis loops for the α-Fe_2O_3 bulk (dashed lines) are also shown for comparison purposes. The values of the magnetization for the α-Fe_2O_3 bulk were divided by seven for clarity.

The *M-H* curves of the α-Fe_2O_3 nanoparticles were explained by assuming that the critical size (d_c) for superparamagnetism was within the size variation of the nanoparticles, i.e., 35~85 nm. In Fig. 2, the existence of both the $T_{M,N}$ and the T_B supported this assumption. The α-Fe_2O_3 nanoparticles with smaller and larger sizes than d_c exhibited different *M-H* behaviors depending on the temperature. The nanoparticle which were larger size than d_c should exhibited a magnetic hysteresis loop above and near the $T_{M,N}$. The antiferromagnetic spin arrangement was not perfect below the $T_{M,N}$, as evidenced by the smooth change in the magnetization near the $T_{M,N}$, because of the vacancies, defects, and spin disorder at the surface of the nanoparticles. Therefore, magnetic hysteresis loops appeared. The magnetic moment and the coercive field decreased with decreasing temperature because of the stabilization of the antiferromagnetic spin arrangement. On the

other hand, the nanoparticle which was smaller than d_c exhibited superparamagnetism. Therefore magnetic hysteresis loops did not appear, but the magnetic moment was quite large above the T_B. Below the T_B, magnetic hysteresis loop appeared because of the spatially frozen moment.

The intriguing *M-H* curves of the α-Fe_2O_3 nanoparticles were explained by the two contributions from the α-Fe_2O_3 nanoparticles with smaller and larger sizes than d_c. For example, the larger magnetization value at 2 T and 140 K compared to 220 K was possibly caused by the additional magnetic moment contribution from the superparamagnetism. The large coercive field at 5 K might have been caused by both the frozen magnetic moment and the antiferromagnetic spins. Additionally, the large remanent magnetization at 5 K might have been caused by the sum of the two contributions from the frozen magnetic moment and the disordered surface spins.

4. Conclusion

The magnetic properties highly crystalline α-Fe_2O_3 nanoparticles with a uniform size and shape were investigated. The critical size for superparamagnetism was within the size distribution of the nanoparticles. The synthetic method and the magnetic properties are currently being investigated for the monodisperse (size variation < 5%) α-Fe_2O_3 nanoparticles with a high crystalline quality.

Acknowledgments

This work was supported by the Korea Research Foundation Grant funded by the Korean Government (MOEHRD) (KRF-2008-313-C00253).

References

[1] G. Schmid, Nanoparticles: From Theory to Application, Wiley-VCH, Weinheim (2004).
[2] Y.-J. Suh, D.-S. Kil, K.-S. Chung, H.-S. Lee, and H. Shao, J. Magnetics **13**, 106 (2008).
[3] F. J. Morin, Phys. Rev. **78**, 819 (1950).
[4] J. O. Artmann, J. C. Murphy, and S. Foner, Phys. Rev. **138A**, 912 (1965).
[5] N. Yamamoto, J. Phys. Soc. Jpn. **24**, 23 (1968).
[6] C. Rath, K. K. Sahu, and S. D. Kulkarni, Appl. Phys. Lett. **75**, 4171 (1999).
[7] D. Jagadeesan, U. Mansoori, P. Mandal, A. Sundaresan, and M. Eswaramoorthy, Angew. Chem. Int. Ed. **47**, 7685 (2008).
[8] L. Suber, D. Fiorani, P. Imperatori, S. Foglia, A. Montone, and R. Zysler, Nanostruct. Mater. **11**, 797 (1999).
[9] Y. S. Koo, K. M. Song, N. Hur, J. H. Jung, T-H. Jang, H. J. Lee, T. Y. Koo, Y. H. Jeong, J. H. Cho, and Y. H. Jo, Appl. Phys. Lett. **94**, 032903 (2009).
[10] J. H. Cho, S. G. Ko, Y. Ahn, and E. J. Choi, J. Magnetics **14**, 124 (2009).
[11] Y. S. Koo, D. H. Kim, and J. H. Jung, J. Korean Phys. Soc. **48**, 677 (2006).
[12] S. Mitra, S. Das, K. Mandal, and S. Chaudhuri, Nanotechnology **18**, 275608 (2007).
[13] X. N. Xu, Y. Wolfus, A. Shaulov, Y. Yeshurun, I. Felner, I. Nowik, Y. Koltypin, and A. Gedanken, J. Appl. Phys. **91**, 4611 (2002).
[14] L. Haibo, G. Jie, Z. Weitao, C. Gang, and Y. Ruihuang, Chinese Sci. Bull. **42**, 344 (1997).
[15] F. Bodker, M. F. Hansen, C. B. Koch, K. Lefmann, and S. Morup, Phys. Rev. B **61**, 6826 (2000).